

# Fully Automated Precision Predictions for Heavy Neutrino Production Mechanisms at Hadron Colliders

Céline Degrande,<sup>1,\*</sup> Olivier Mattelaer,<sup>1,†</sup> Richard Ruiz,<sup>1,‡</sup> and Jessica Turner<sup>1,§</sup>

<sup>1</sup>*Institute for Particle Physics Phenomenology, Department of Physics, Durham University, Durham DH1 3LE, U.K.*

(Dated: September 13, 2016)

Motivated by TeV-scale neutrino mass models, we propose a systematic treatment of heavy neutrino ( $N$ ) production at hadron colliders. Our simple and efficient modeling of the vector boson fusion (VBF)  $W^\pm\gamma \rightarrow N\ell^\pm$  and  $N\ell^\pm + nj$  signal definitions resolve collinear and soft divergences that have plagued past studies, and is applicable to other color-singlet processes, e.g., associated Higgs ( $W^\pm h$ ), sparticle ( $\tilde{\ell}^\pm\tilde{\nu}_\ell$ ), and charged Higgs ( $h^{\pm\pm}h^\mp$ ) production. We present, for the first time, a comparison of all leading  $N$  production modes, including both gluon fusion (GF)  $gg \rightarrow Z^*/h^* \rightarrow N\tilde{\nu}_\ell^{(-)}$  and VBF. We obtain fully differential results up to next-to-leading order (NLO) in QCD accuracy using a Monte Carlo tool chain linking FeynRules, NLOCT, and MadGraph5\_aMC@NLO. Associated model files are publicly available. At the 14 TeV LHC, the leading order GF rate is small and comparable to the NLO  $N\ell^\pm + 1j$  rate; at a future 100 TeV Very Large Hadron Collider, GF dominates for  $m_N = 300 - 1500$  GeV, beyond which VBF takes lead.

PACS numbers: 14.60.St, 12.38.-t

## INTRODUCTION

The origin of neutrino masses  $m_\nu$  that are tiny compared to all other fermion masses is a broad issue in particle physics, cosmology, and astrophysics. Nonzero  $m_\nu$  imply the existence of new particles [1], but more generally, physics beyond the Standard Model (BSM) that may be observable at current and future experiments. Extended neutrino mass models [2–10] based on the Type I [11–20], Inverse [21–23], and Linear See-saw Mechanisms [24, 25], feature heavy mass eigenstates  $N_i$  that couple to electroweak (EW) bosons via mixing with left-handed (LH) neutrinos  $\nu_L$ . In these TeV-scale scenarios, active-sterile mixing can be as large as  $|V_{\ell N_i}| \sim 10^{-3} - 10^{-2}$ , and consistent with oscillation and EW data [26–28], as well as direct searches by the Large Hadron Collider (LHC) experiments [29–31]. Thus, if kinematically accessible, hadron colliders can produce heavy neutrinos that decay to lepton number- and/or flavor-violating final states with observable rates.

For heavy  $N$  masses  $m_N$  above the EW scale, a systematic comparison of all leading single  $N$  production modes cataloged in [32, 33] has never been performed. Most investigations focus on the charge current (CC) Drell-Yan (DY) process [2, 26, 32, 34–36], as shown in Fig. 1(a),

$$q\bar{q} \rightarrow W^* \rightarrow N\ell^\pm, \quad q \in \{u, c, d, s, b\}, \quad (1)$$

and has recently been found to be subleading in parts of this mass regime [37, 38]. Missing in most analyses is the gluon fusion (GF) channel [37], which proceeds at leading order (LO) through quark triangles in Fig. 1(b),

$$gg \rightarrow h^*/Z^* \rightarrow N\tilde{\nu}_\ell^{(-)}. \quad (2)$$

Variants of Eq. (2) have been studied elsewhere [39, 40]. Formally, GF is a finite next-to-next-to-leading order in QCD correction to the neutral current (NC) DY process

$$q\bar{q} \rightarrow Z^* \rightarrow N\tilde{\nu}_\ell^{(-)}. \quad (3)$$

Recent analyses have investigated the sizable EW vector boson fusion (VBF) process [38, 41–46]:

$$q_1 q_2 \xrightarrow{W\gamma+WZ \text{ Fusion}} N\ell^\pm q'_1 q'_2, \quad (4)$$

and subleading CC DY with  $n \geq 1$  QCD jets [41, 46, 47]:

$$pp \rightarrow W^* + nj \rightarrow N\ell^\pm + nj, \quad p, j \in \{q, g\}, \quad (5)$$

but with conflicting results. The last two processes are plagued by soft and collinear poles in  $s$ - and  $t$ -channel exchanges of massless gauge bosons, issues usually associated with perturbative QCD, and require care [38, 48]. E.g., inadequately regulated divergences are responsible for the overestimated cross sections claimed in [41, 43, 46, 47]

We introduce a treatment that resolves all these issues. Our results have widespread implications for SM and BSM physics: the prescriptions for Eqs. (4) and (5) are applicable to, among other processes, associated Higgs ( $W^\pm h$ ), sparticle ( $\tilde{\ell}^\pm\tilde{\nu}_\ell$ ), and charged Higgs ( $h^{\pm\pm}h^\mp$ ) production. To date, our study is the most accurate and comprehensive presentation of heavy  $N$  production mechanisms at colliders. It represents the first time properties of infrared and collinear (IRC) safety have been so rigorously imposed in this context, particularly to VBF. Furthermore, we obtain modest next-to-leading order (NLO) in QCD corrections, demonstrating the stability of our approach.

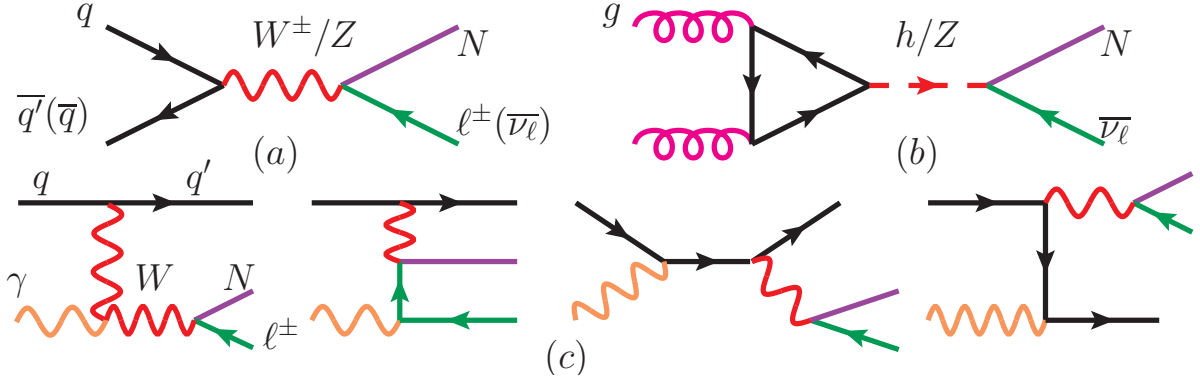


FIG. 1: Heavy neutrino production via (a) charge (neutral) current Drell-Yan, (b) gluon fusion, and (c)  $W\gamma$  fusion.

We guarantee the perturbativity of the VBF process by factorizing and resumming the  $t$ -channel  $\gamma$  into a DGLAP-evolved parton distribution function (PDF). Using a  $\gamma$ -PDF, one considers instead, as shown in Fig. 1(c),

$$q \gamma \rightarrow N \ell^\pm q'. \quad (6)$$

$WZ$  fusion is subleading and can be neglected [38]. We regularize Eq. (5) by imposing transverse momentum ( $p_T$ ) cuts consistent with Collins-Soper-Sterman (CSS)  $p_T$ -resummation [49]. Our Monte Carlo (MC) framework allows us to compute fully differential Feynman diagrams up to one loop, and therefore GF at LO and the remaining processes at NLO; only Eq. (1) has been evaluated before at NLO [50, 51].

At the 14 TeV LHC, the CC DY channel prevails for  $N$  masses  $m_N = 150 - 850$  GeV; above this, the VBF cross section is larger. However, due to the  $gg$  luminosity increase, GF is the leading mechanism at a hypothetical future 100 TeV Very Large Hadron Collider (VLHC) for  $m_N = 300 - 1500$  GeV; at higher  $m_N$ , VBF dominates.

We now introduce our theoretical model, computation procedure, and signal definition prescription. After presenting and discussing results, we conclude.

## HEAVY NEUTRINO MODEL

For  $i$  ( $m$ ) = 1, ..., 3, LH (light) states and  $j$  ( $m'$ ) = 1, ...,  $n$ , right-handed (heavy) states, chiral neutrinos can be expanded into mass eigenstates by the rotation

$$\begin{pmatrix} \nu_{Li} \\ N_{Rj}^c \end{pmatrix} = \begin{pmatrix} U_{3 \times 3} & V_{3 \times n} \\ X_{n \times 3} & Y_{n \times n} \end{pmatrix} \begin{pmatrix} \nu_m \\ N_{m'}^c \end{pmatrix}. \quad (7)$$

After rotating the charged leptons into the mass basis, which we take to be the identity matrix for simplicity,  $U_{3 \times 3}$  is the observed light neutrino mixing matrix and  $V_{3 \times n}$  parameterizes active-heavy mixing. In the notation

of [26], the flavor state  $\nu_\ell$  in the mass basis is

$$\nu_\ell = \sum_{m=1}^3 U_{\ell m} \nu_m + \sum_{m'=1}^n V_{\ell m'} N_{m'}^c. \quad (8)$$

For simplicity, we consider only one heavy mass eigenstate, labeled by  $N$ . This does not affect our conclusions. The interaction Lagrangian with EW bosons is then

$$\begin{aligned} \mathcal{L}_{\text{Int.}} = & - \frac{g}{\sqrt{2}} W_\mu^+ \sum_{\ell=e}^{\tau} \sum_{m=1}^3 \bar{\nu}_m U_{\ell m}^* \gamma^\mu P_L \ell^- \\ & - \frac{g}{\sqrt{2}} W_\mu^+ \sum_{\ell=e}^{\tau} \bar{N}^c V_{\ell N}^* \gamma^\mu P_L \ell^- \\ & - \frac{g}{2 \cos \theta_W} Z_\mu \sum_{\ell=e}^{\tau} \sum_{m=1}^3 \bar{\nu}_m U_{\ell m}^* \gamma^\mu P_L \nu_\ell \\ & - \frac{g}{2 \cos \theta_W} Z_\mu \sum_{\ell=e}^{\tau} \bar{N}^c V_{\ell N}^* \gamma^\mu P_L \nu_\ell \\ & - \frac{gm_N}{2M_W} h \sum_{\ell=e}^{\tau} \bar{N}^c V_{\ell N}^* P_L \nu_\ell + \text{H.c.} \end{aligned} \quad (9)$$

Precise values of  $V_{\ell N}$  are model-dependent and are constrained by oscillation and collider experiments, tests of lepton universality, and  $0\nu\beta\beta$ -decay [26–28]. However,  $V_{\ell N}$  factorize in  $N$  production cross sections such that

$$\sigma(pp \rightarrow N X) = |V_{N\ell}|^2 \times \sigma_0(pp \rightarrow N X), \quad (10)$$

where  $\sigma_0$  is a model-independent “bare” cross section in which one sets  $|V_{N\ell}| = 1$ . Hence, our results are applicable to various heavy neutrino models.

## COMPUTATIONAL SETUP

We implement the above Lagrangian with Goldstone boson couplings in the Feynman gauge into FeynRules

(FR) 2.3.10 [52, 53]. QCD renormalization and  $R_2$  rational counterterms are calculated with NLOCT 1.02 (prepackaged in FR) [54] and FeynArts 3.8 [55]. Feynman rules are collected into a universal output file (UFO) [56] and is available publicly [57]. We obtain fully differential results using MadGraph5\_aMC@NLO 2.3.3 [58]. SM inputs are taken from the 2014 Particle Data Group [59]:

$$\begin{aligned}\alpha_{\overline{\text{MS}}}(M_Z) &= 1/127.940, & M_Z &= 91.1876 \text{ GeV}, \\ \sin_{\overline{\text{MS}}}^2(\theta_W) &= 0.23126.\end{aligned}\quad (11)$$

We assume five massless quarks, take the Cabbibo-Kobayashi-Masakawa (CKM) matrix to be diagonal with unit entries, and use the NLO NNPDF2.3 QED PDF (lhaid:244600) [60], which features a  $\gamma$ -PDF with both elastic and inelastic components, at collider energies of  $\sqrt{s} = 14$  and 100 TeV. We extract  $\alpha_s(\mu_r^2)$  from the PDFs.

### INFRARED- AND COLLINEAR-SAFE HADRON COLLIDER SIGNAL DEFINITIONS

To consistently compare channels and colliders, we follow the 2013 Snowmass recommendations [61] and evaluate cross sections assuming the same fiducial acceptance. In practice, however, one tunes cuts to specific colliders and final states. Jet and charged lepton pseudorapidities ( $\eta^{j,\ell}$ ) and charged lepton  $p_T$  are required to satisfy [61]:

$$|\eta^{j,\ell}| < 2.5, \quad p_T^\ell > 20 \text{ GeV}.\quad (12)$$

QCD radiation in Eq. (5) gives rise to fixed order (FO) cross sections that scale as powers of  $\log(Q^2/q_T^2)$ :

$$\sigma(pp \rightarrow N\ell^\pm + nj) \sim \sum_k^n \alpha_s^k(Q^2) \log^{(2k-1)}\left(\frac{Q^2}{q_T^2}\right).\quad (13)$$

$Q \sim m_N$  is the scale of the hard scattering process and  $q_T \equiv \sum_k^n p_{T,k}^j$  is the  $(N\ell)$ -system's transverse momentum, which equals the sum of all jet  $p_T$ . The perturbativity of these logarithms for TeV-scale leptons was studied in [48]. In the CSS  $p_T$ -resummation formalism [49], FO results are trustworthy when  $\alpha_s(Q^2)$  is perturbative, with  $\Lambda_{\text{QCD}} = 0.2 \text{ GeV}$ , and  $q_T$  is comparable to  $Q$ :

$$\log \frac{Q}{\Lambda_{\text{QCD}}} \gg 1 \quad \text{and} \quad \log^2 \frac{Q}{q_T} \lesssim \log \frac{Q}{\Lambda_{\text{QCD}}}.\quad (14)$$

Imposing  $Q = m_N$ , jets in Eq. (13) must satisfy

$$\sum_k^n p_{T,k}^j \gtrsim m_N \times e^{-\sqrt{\log(m_N/\Lambda_{\text{QCD}})}}.\quad (15)$$

Taking for example  $n = 1$  and  $m_N$  up to 1 (1.5) TeV, the mass range of interest at 14 (100) TeV, this translates to

$$p_T^j \gtrsim 55 \text{ (80) GeV}.\quad (16)$$

Weaker  $p_T^j$  cuts lead to artificially large logarithms and overestimated cross sections in Eq. (13). We cluster jets with FastJet [62, 63] using the anti- $k_T$  algorithm [64] with a separation parameter of  $\Delta R = 0.4$ . For differential events, we parton shower (PS) with Pythia 8.212 [65].

We equate the factorization and renormalization scales to half the sum over final-state transverse masses (dynamical\_scale\_choice=3 in MadGraph5\_aMC@NLO):

$$\mu_f, \mu_r, \mu_0 = \sum_{k=N,\ell,\text{jets}} \frac{m_{T,k}}{2} = \frac{1}{2} \sum_k \sqrt{m_k^2 + p_{T,k}^2}.\quad (17)$$

We quantify the scale dependence by varying it over

$$0.5 \leq \mu/\mu_0 \leq 2.\quad (18)$$

In our framework, the CC DY rate at NLO can be calculated via the MadGraph5\_aMC@NLO commands:

```
> import model HeavyN_NLO
> define p = u c d s b u~ c~ d~ s~ b~ g
> define j = p
> define mu = mu+ mu-
> generate p p > n2 mu [QCD]
> output PP_N1_NLO; launch;
```

Similarly, the inclusive NC DY at NLO is calculated by

```
> define vv = vm vm~
> generate p p > n2 vv [QCD]
> output PP_Nv_NLO; launch;
```

and the inclusive CC DY + 1j NLO rate by

```
> generate p p > n2 mu j QED=2 QCD=1 [QCD]
> output PP_N11j_NLO; launch;
```

GF is a loop-induced process, which are only recently [66] supported by MadGraph5\_aMC@NLO. Such fully automated computations at NLO are unavailable since the two-loop technology does not currently exist. We therefore perform the LO calculation matched and merged with up to one additional jet via the MLM scheme [67]. We discard loops that are actually virtual corrections to the DY process and keep only diagrams where gluons do not appears in the loop. The inclusive, unmatched LO GF rate can be calculated with

```
> generate g g > n2 vv [QCD]
> output GGF_Nv_LO; launch;
```

Note that the  $h^*/Z^*$  interference vanishes due to  $C$ -invariance/Furry's theorem and the (anti-) symmetric nature of the residual  $h$  ( $Z$ ) coupling [37, 68].

The difficulty in modeling  $W\gamma$  fusion stems from the  $t$ -channel photon propagator, which, like Eq. (13) for  $N\ell^\pm + nj$ , gives rise to logarithms of the form [38]

$$d\sigma(q_1 q_2 \rightarrow N\ell^\pm q'_1 q'_2) \sim \log\left(\frac{m_N^2}{M_W^2}\right) \log\left(\frac{m_N^2}{p_T^{j,\gamma^2}}\right).\quad (19)$$

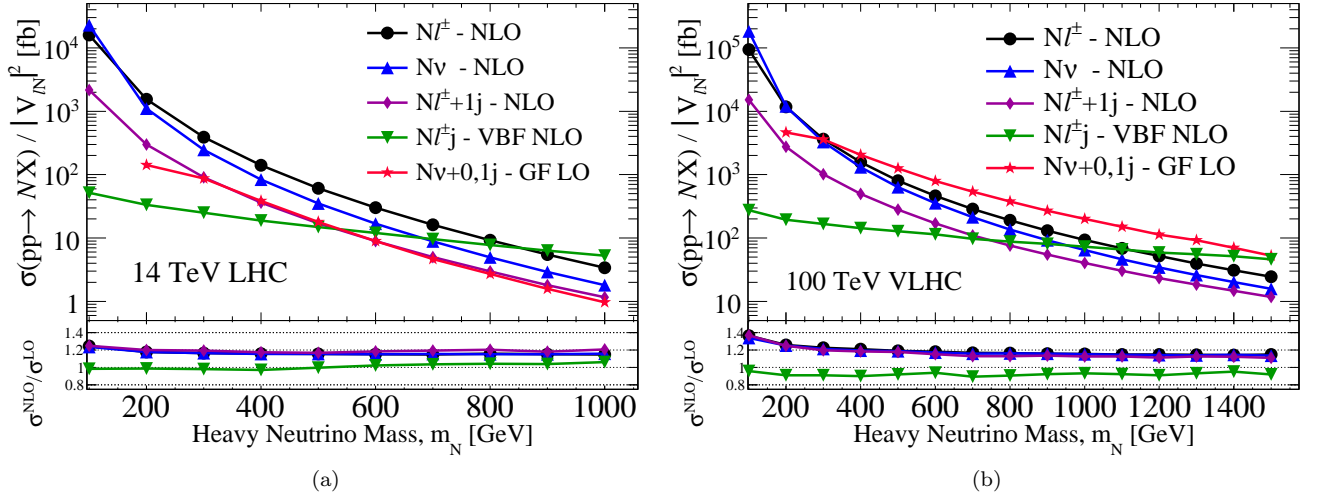


FIG. 2: Heavy  $N$  NLO production rate in (a) 14 and (b) 100 TeV  $pp$  collisions as a function of  $m_N$ , divided by active-heavy mixing  $|V_{\ell N}|^2$ , for the inclusive CC (circle) and NC (triangle) DY,  $N\ell^\pm + 1j$  (diamond), and VBF (upside-down triangle) processes, as well as the LO GF process matched up to  $1j$  (star). Lower: Ratio of NLO and LO rates.

Here,  $p_T^{j\gamma}$  is the  $p_T$  of the jet associated with the photon exchange. However, consistent treatment of Eq. (19) dictates  $p_T^j$  cuts excessive for  $\gamma$ -initiated processes. A resolution is to collinearly factorize and resum the photon piece into a DGLAP-evolved  $\gamma$ -PDF, consider instead

$$q \gamma \rightarrow N \ell^\pm q', \quad (20)$$

and evolve the PDF to the hard scattering scale. One loses the ability to efficiently tag a second forward/backward jet but gains a large (logarithmic) total rate enhancement [38]. Eq. (20) is realization of the structure function approach to VBF [69]. Formally, the  $N\ell^\pm qq'$  channel can be recovered by performing the ACOT-like jet matching explicitly as in [38] or evaluating the NLO in QED corrections to Eq. (20). For VBF, we impose the  $\eta^j, p_T^j$  cuts of [38]:

$$|\eta^{j\text{VBF}}| < 4.5, \quad p_T^{j\text{VBF}} > 30 \text{ GeV}. \quad (21)$$

Collinear poles associated with  $t$ -channel  $\ell$  exchange emerge in Eq. (20) but are regulated by cuts in Eq. (12). The process at NLO in QCD is simulated by

```
> define q = u c d s b u~ c~ d~ s~ b~
> generate q a > n2 mu q QED=3 QCD=0 [QCD]
> add process a q > n2 mu q QED=3 QCD=0 [QCD]
> output PP_VBF_NLO; launch;
```

## RESULTS

As a function of  $m_N$ , we present in Fig. 2 the (a) 14 and (b) 100 TeV heavy  $N$  production rates, divided by active-heavy mixing. At NLO are the CC DY (circle), NC DY (triangle),  $N\ell^\pm + 1j$  (diamond), and VBF (upside-down

triangle) processes; at LO is GF (star). The lower panel shows the NLO-to-LO ratio, the so-called NLO  $K$ -factor:

$$K^{\text{NLO}} \equiv \sigma^{\text{NLO}}/\sigma^{\text{LO}}. \quad (22)$$

For select  $m_N$ , we summarize our results in Tb. I.

For  $m_N = 100 - 1000$  (100 - 1500) GeV, NLO production rates for the DY channels at 14 (100) TeV span:

$$\text{CC DY} : 3.4 \text{ fb} - 16 \text{ pb} \quad (25 \text{ fb} - 94 \text{ pb}), \quad (23)$$

$$+1j : 1.2 \text{ fb} - 2.1 \text{ pb} \quad (12 \text{ fb} - 15 \text{ pb}), \quad (24)$$

$$\text{NC DY} : 1.8 \text{ fb} - 23 \text{ pb} \quad (16 \text{ fb} - 180 \text{ pb}), \quad (25)$$

with corresponding scale uncertainties:

$$\text{CC DY} : \pm 1 - 5\% \quad (\pm 1 - 11\%), \quad (26)$$

$$+1j : \pm 2 - 6\% \quad (\pm 1 - 7\%), \quad (27)$$

$$\text{NC DY} : \pm 1 - 5\% \quad (\pm 1 - 13\%), \quad (28)$$

and nearly identical  $K$ -factors:

$$\text{CC DY, } +1j, \text{ NC} : 1.15 - 1.25 \quad (1.11 - 1.37). \quad (29)$$

The increase over LO rates is due to the opening of the  $gq^{(-)}$  and  $gg$  channels for the DY and  $+1j$  processes, respectively. Since the gluon PDF is largest at Bjorken- $x \sim m_N/\sqrt{s} \ll 1$ , the biggest change is at low  $m_N$ . We find that DY+2j  $K$ -factors are consistent with high-mass SM DY in SHERPA [70]. The modest size of these corrections validates our approach.

The VBF rate, uncertainty, and  $K$ -factor span

$$\sigma_{\text{VBF}} : 5.3 - 52 \text{ fb} \quad (46 - 280 \text{ fb}), \quad (30)$$

$$\delta\sigma_{\text{VBF}}/\sigma : \pm 5 - 11\% \quad (\pm 9 - 14\%), \quad (31)$$

$$K_{\text{VBF}} : 0.98 - 1.06 \quad (0.90 - 0.96). \quad (32)$$

$\sqrt{s}$	14 TeV						100 TeV					
	500 GeV			1 TeV			500 GeV			1 TeV		
$m_N$	LO	NLO	$K$	LO	NLO	$K$	LO	NLO	$K$	LO	NLO	$K$
$\sigma /  V_{\ell N} ^2$ [fb]	LO	NLO	$K$	LO	NLO	$K$	LO	NLO	$K$	LO	NLO	$K$
CC DY	52.8	61.1 <sup>+1.9%</sup> <sub>-1.6%</sub>	1.16	2.96	3.40 <sup>+2.2%</sup> <sub>-2.4%</sub>	1.15	674	804 <sup>+2.4%</sup> <sub>-3.4%</sub>	1.19	80.8	93.5 <sup>+1.4%</sup> <sub>-1.6%</sub>	1.16
NC DY	30.4	35.2 <sup>+1.8%</sup> <sub>-1.5%</sub>	1.16	1.56	1.81 <sup>+2.4%</sup> <sub>-2.5%</sub>	1.16	537	638 <sup>+2.5%</sup> <sub>-3.6%</sub>	1.19	55.9	64.4 <sup>+1.5%</sup> <sub>-1.7%</sub>	1.15
CC DY+1j	14.5	17.0 <sup>+3.2%</sup> <sub>-4.5%</sub>	1.17	0.970	1.17 <sup>+4.0%</sup> <sub>-5.6%</sub>	1.21	238	280 <sup>+2.1%</sup> <sub>-3.0%</sub>	1.18	35.8	40.3 <sup>+2.0%</sup> <sub>-2.4%</sub>	1.13
GF+0, 1j	17.9	...	...	0.967	...	...	1,260	...	...	200	...	...
VBF	15.0	15.0 <sup>+7.8%</sup> <sub>-7.3%</sub>	0.998	4.97	5.28 <sup>+6.3%</sup> <sub>-5.4%</sub>	1.06	139	128 <sup>+12.3%</sup> <sub>-11.7%</sub>	0.918	78.4	73.2 <sup>+10.0%</sup> <sub>-9.7%</sub>	0.932

TABLE I: LO and NLO heavy neutrino production rates, divided by active-heavy mixing  $|V_{\ell N}|^2$ , and scale dependence (%) in  $\sqrt{s} = 14$  and 100 TeV  $pp$  collisions for representative heavy neutrino masses  $m_N$ .

Due to collinear logarithmic enhancements, the VBF rate falls slower with  $m_N$  than  $s$ -channel mechanisms. At 14 (100) TeV, the VBF rate surpasses the CC DY rate at  $m_N \approx 850$  (1100) GeV. This somewhat differs from [38] and can be traced to the different  $\gamma$ -PDFs used: at large (small) scales of  $\tau = m_N^2/s$ , the  $q\gamma$  luminosity here is larger (smaller) than in [38], leading to VBF overtaking the DY CC at smaller (larger) values of  $m_N$ . However, present-day  $\gamma$ -PDF uncertainties are sizable [60, 71].

For all NLO processes, our scale dependence peaks at  $m_N = 100 - 200$  GeV; it is attributed, in part, to the large gluon PDF uncertainty at small  $x$ .

For  $m_N \geq 200$  GeV, the matched LO GF rate spans

$$\sigma_{\text{GF}} : 1.0 \text{ fb} - 0.1 \text{ pb} \quad (55 \text{ fb} - 4.7 \text{ pb}). \quad (33)$$

At 14 TeV, the rate is comparable to  $N\ell + 1j$  at NLO. Though both obey  $s$ -channel scaling, the similarities are accidental and due to phase space cuts. GF is roughly  $0.1 - 0.3 \times$  the CC DY rate. At 100 TeV, the situation is qualitatively different: Due to  $gg$  luminosity increase at 100 TeV, which grows  $\sim 10 \times$  more than the DY luminosity [72], GF jumps to  $0.4 - 2 \times$  the CC DY rate, becoming the dominant production mode for  $m_N = 300 - 1500$  GeV. Beyond this  $m_N$ , VBF is largest. We observe that Higgs and  $Z$  diagrams contribute about equally at large  $m_N$ . Our matched results are consistent with the unmatched calculation of [37].

### NLO+PS Kinematics at 14 TeV

We now consider the differential distribution for the processes in Fig. 1 but focus largely on the VBF channel. The kinematics of heavy lepton production from DY currents at NLO and NLO+Leading Log(recoil) was studied in [48]. There, the differential NLO  $K$ -factors, defined as

$$K_{\mathcal{O}}^{\text{NLO}} \equiv \frac{d\sigma^{\text{NLO}}/d\mathcal{O}}{d\sigma^{\text{LO}}/d\mathcal{O}} \quad (34)$$

for observable  $\mathcal{O}$ , were analytically shown to be flat in the leading regions of phase space. In these regions, NLO contributions are dominated by soft initial-state radiation, which generically factorize for DY processes. We

confirm the flatness of  $K_{\mathcal{O}}^{\text{NLO+PS}}$  for the DY channels, including for complex observables such as cluster mass in the  $N\ell \rightarrow 3\ell\nu$  final state.

The phenomenology of the GF channel has not been previously studied. It is beyond the scope of this investigation to do so here and will be presented elsewhere.

At  $\sqrt{s} = 14$  TeV and representative neutrino mass  $m_N = 500$  GeV, the LO distributions for the  $W\gamma$  fusion process was studied in Ref. [38]. For the first time, we show in Fig. 3 the NLO+PS (dash) and LO+PS (solid)-accurate distributions with respect to (a,c)  $p_T$  and (b,d) rapidity ( $y$ ) of the (a,b)  $N$ - and (c,d)  $(N\ell)$ -systems.  $K_{\mathcal{O}}^{\text{NLO+PS}}$  is shown in the lower panel. For the two system, but particularly the  $(N\ell)$ -system, we observe a net migration at NLO+PS of events from the lowest  $p_T$  bins resulting in  $K_{p_T}^{\text{NLO+PS}} < 1$  for these bins. At high  $p_T$ ,  $K_{p_T}^{\text{NLO+PS}}$  quickly converges to unity from above. In the rapidity distributions, we observe a similar, but more pronounced, migration of events from large  $y$  to smaller values, consistent with shifts to larger  $p_T$ . The charged lepton  $p_T$  and  $\eta$  distributions (not shown) demonstrate little sensitivity to  $\mathcal{O}(\alpha_s)$  corrections. However, as VBF is dominated by  $\gamma \rightarrow \ell$  splittings [38], one does not expect such sensitivity to QCD radiation until  $\mathcal{O}(\alpha^2\alpha_s)$ . Though numerically less significant, we find that the NLO corrections to the VBF distributions are qualitatively different than those of DY-like systems: whereas differential  $K$ -factors for DY processes tend to remain flat and above unity, QCD corrections for  $W\gamma$  fusion tend to depopulate low- $p_T$ /forward regions of phase space and populate high- $p_T$ /central regions. This results in  $K$ -factors both above and below unity.

## SUMMARY AND CONCLUSION

The origin of light neutrino masses remains elusive. Extended neutrino mass models predict the existence TeV-scale heavy neutrinos  $N_i$  that may be discovered at current or future collider experiments.

We propose a systematic treatment of  $N$  production mechanisms at hadron colliders, and provide instructions for building IRC-safe VBF and  $N\ell^\pm + nj$  signal defini-

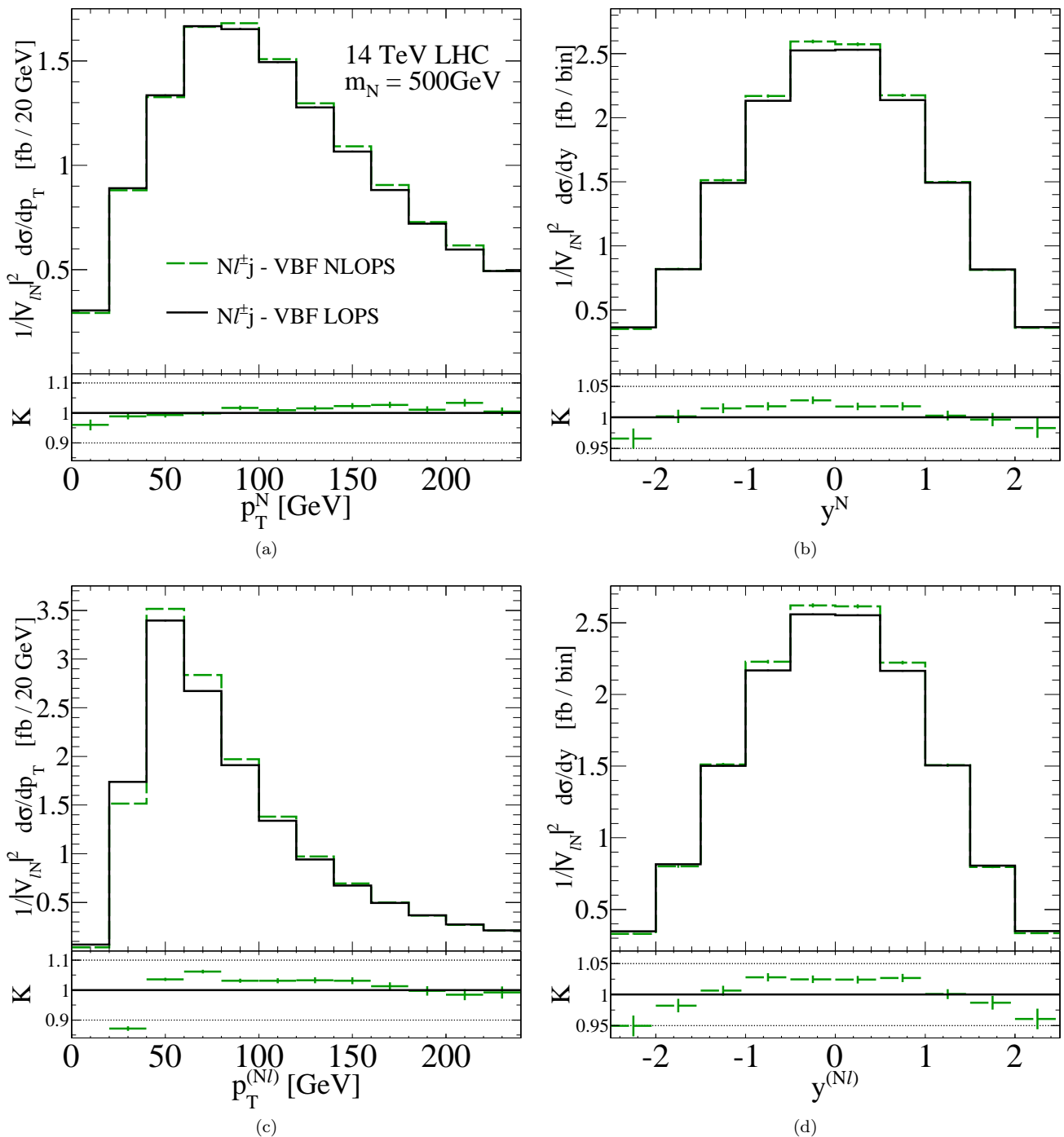


FIG. 3: Differential distributions with respect to (a,c)  $p_T$  and (b,d)  $y$  of (a,b)  $N$  and (c,d) the  $(N\ell)$  system at NLOPS (dash) and LOPS (solid) accuracy in VBF at 14 TeV LHC for representative  $m_N$  500 GeV. Lower: Ratio of NLOPS and LOPS rates.

tions. The prescription remedies issues that have plagued past analyses, and is applicable to a number of other SM and BSM processes. We report modest NLO corrections, demonstrating the perturbative stability of our approach. We present also the first NLOPS-accurate differential distributions for the  $W\gamma$  VBF process. We observe nontrivial differential  $K$ -factors below and above unity.

In a model-independent fashion, we present for the first time a comparison of all leading single  $N$  production modes at  $\sqrt{s} = 14$  and 100 TeV. Fully differential results up to NLO in QCD accuracy are obtained through a MC tool chain linking FeynRules, NLOCT, and MadGraph5\_aMC@NLO. Associated model files are publicly available [57].

*Acknowledgements: D. Alva, L. Brenner, B. Fuks, T. Han, V. Hirschi, J. Rojo, S. Pascoli, C. Tamarit, C. Weiland are thanked for discussions and readings of the manuscript. S. Kuttimalai and T. Morgan are thanked for their numerical checks. This work has been supported by Science and Technology Facilities Council (STFC), the European Unions Horizon 2020 research, and innovation programme under the Marie Skłodowska-Curie grant agreements No 690575 and 674896. OM and CD are Durham International Junior Research Fellow.*

\* Electronic address: [celine.degrande@durham.ac.uk](mailto:celine.degrande@durham.ac.uk)

† Electronic address: [o.p.c.mattelaer@durham.ac.uk](mailto:o.p.c.mattelaer@durham.ac.uk)

‡ Electronic address: [richard.ruiz@durham.ac.uk](mailto:richard.ruiz@durham.ac.uk)

§ Electronic address: [jessica.turner@durham.ac.uk](mailto:jessica.turner@durham.ac.uk)

- [1] E. Ma, Phys. Rev. Lett. **81**, 1171 (1998)
- [2] A. Pilaftsis, Z. Phys. C **55**, 275 (1992) doi:10.1007/BF01482590
- [3] J. Kersten and A. Y. Smirnov, Phys. Rev. D **76**, 073005 (2007) doi:10.1103/PhysRevD.76.073005
- [4] P. H. Gu, M. Hirsch, U. Sarkar and J. W. F. Valle, Phys. Rev. D **79**, 033010 (2009) doi:10.1103/PhysRevD.79.033010
- [5] P. S. B. Dev and R. N. Mohapatra, Phys. Rev. D **81**, 013001 (2010) doi:10.1103/PhysRevD.81.013001
- [6] H. Zhang and S. Zhou, Phys. Lett. B **685**, 297 (2010) doi:10.1016/j.physletb.2010.02.015
- [7] R. Adhikari and A. Raychaudhuri, Phys. Rev. D **84**, 033002 (2011) doi:10.1103/PhysRevD.84.033002
- [8] C. Y. Chen, P. S. B. Dev and R. N. Mohapatra, Phys. Rev. D **88**, 033014 (2013) doi:10.1103/PhysRevD.88.033014
- [9] C. H. Lee, P. S. Bhupal Dev and R. N. Mohapatra, Phys. Rev. D **88** (2013) no.9, 093010 doi:10.1103/PhysRevD.88.093010
- [10] P. S. Bhupal Dev, C. H. Lee and R. N. Mohapatra, J. Phys. Conf. Ser. **631**, no. 1, 012007 (2015) doi:10.1088/1742-6596/631/1/012007
- [11] P. Minkowski, Phys. Lett. B **67**, 421 (1977).
- [12] T. Yanagida, Conf. Proc. C **7902131**, 95 (1979).
- [13] P. Van Nieuwenhuizen and D. Z. Freedman, Amsterdam, Netherlands: North-holland (1979) 341p
- [14] P. Ramond, hep-ph/9809459.
- [15] S. L. Glashow, NATO Sci. Ser. B **59**, 687 (1980).
- [16] R. N. Mohapatra and G. Senjanovic, Phys. Rev. Lett. **44**, 912 (1980).
- [17] M. Gell-Mann, P. Ramond and R. Slansky, Conf. Proc. C **790927**, 315 (1979)
- [18] J. Schechter and J. W. F. Valle, Phys. Rev. D **22**, 2227 (1980).
- [19] R. E. Shrock, Phys. Rev. D **24**, 1232 (1981).
- [20] J. Schechter and J. W. F. Valle, Phys. Rev. D **25**, 774 (1982).
- [21] R. N. Mohapatra, Phys. Rev. Lett. **56**, 561 (1986). doi:10.1103/PhysRevLett.56.561
- [22] R. N. Mohapatra and J. W. F. Valle, Phys. Rev. D **34**, 1642 (1986). doi:10.1103/PhysRevD.34.1642
- [23] J. Bernabeu, A. Santamaria, J. Vidal, A. Mendez and J. W. F. Valle, Phys. Lett. B **187**, 303 (1987). doi:10.1016/0370-2693(87)91100-2
- [24] E. K. Akhmedov, M. Lindner, E. Schnapka and J. W. F. Valle, Phys. Lett. B **368**, 270 (1996) doi:10.1016/0370-2693(95)01504-3
- [25] E. K. Akhmedov, M. Lindner, E. Schnapka and J. W. F. Valle, Phys. Rev. D **53**, 2752 (1996) doi:10.1103/PhysRevD.53.2752
- [26] A. Atre, T. Han, S. Pascoli and B. Zhang, JHEP **0905**, 030 (2009)
- [27] S. Antusch and O. Fischer, JHEP **1410**, 094 (2014) doi:10.1007/JHEP10(2014)094
- [28] A. de Gouvea and A. Kobach, Phys. Rev. D **93**, no. 3, 033005 (2016) doi:10.1103/PhysRevD.93.033005
- [29] R. Aaij *et al.* [LHCb Collaboration], Phys. Rev. Lett. **112**, no. 13, 131802 (2014) doi:10.1103/PhysRevLett.112.131802 [arXiv:1401.5361 [hep-ex]].
- [30] G. Aad *et al.* [ATLAS Collaboration], JHEP **1507**, 162 (2015) doi:10.1007/JHEP07(2015)162 [arXiv:1506.06020 [hep-ex]].
- [31] V. Khachatryan *et al.* [CMS Collaboration], JHEP **1604**, 169 (2016) doi:10.1007/JHEP04(2016)169 [arXiv:1603.02248 [hep-ex]].
- [32] W. Y. Keung and G. Senjanovic, Phys. Rev. Lett. **50**, 1427 (1983). doi:10.1103/PhysRevLett.50.1427
- [33] A. Datta, M. Guchait and A. Pilaftsis, Phys. Rev. D **50**, 3195 (1994) doi:10.1103/PhysRevD.50.3195
- [34] T. Han and B. Zhang, Phys. Rev. Lett. **97**, 171804 (2006) doi:10.1103/PhysRevLett.97.171804
- [35] F. del Aguila, J. A. Aguilar-Saavedra and R. Pittau, J. Phys. Conf. Ser. **53**, 506 (2006) doi:10.1088/1742-6596/53/1/032
- [36] F. del Aguila, J. A. Aguilar-Saavedra and R. Pittau, JHEP **0710**, 047 (2007) doi:10.1088/1126-6708/2007/10/047
- [37] A. G. Hessler, A. Ibarra, E. Molinaro and S. Vogl, Phys. Rev. D **91**, no. 11, 115004 (2015) doi:10.1103/PhysRevD.91.115004
- [38] D. Alva, T. Han and R. Ruiz, JHEP **1502**, 072 (2015)
- [39] B. Batell and M. McCullough, Phys. Rev. D **92**, no. 7, 073018 (2015) doi:10.1103/PhysRevD.92.073018
- [40] P. S. Bhupal Dev, R. Franceschini and R. N. Mohapatra, Phys. Rev. D **86**, 093010 (2012) doi:10.1103/PhysRevD.86.093010
- [41] P. S. B. Dev, A. Pilaftsis and U. k. Yang, Phys. Rev. Lett. **112**, no. 8, 081801 (2014) doi:10.1103/PhysRevLett.112.081801
- [42] G. Bambhaniya, S. Khan, P. Konar and T. Mondal, Phys. Rev. D **91**, no. 9, 095007 (2015) doi:10.1103/PhysRevD.91.095007
- [43] F. F. Deppisch, P. S. Bhupal Dev and A. Pilaftsis, New J. Phys. **17**, no. 7, 075019 (2015) doi:10.1088/1367-2630/17/7/075019
- [44] J. N. Ng, A. de la Puente and B. W. P. Pan, JHEP **1512**, 172 (2015) doi:10.1007/JHEP12(2015)172
- [45] E. Arganda, M. J. Herrero, X. Marcano and C. Weiland, Phys. Lett. B **752**, 46 (2016) doi:10.1016/j.physletb.2015.11.013
- [46] A. Das and N. Okada, Phys. Rev. D **93**, no. 3, 033003 (2016) doi:10.1103/PhysRevD.93.033003
- [47] A. Das, P. S. Bhupal Dev and N. Okada, Phys. Lett. B **735**, 364 (2014) doi:10.1016/j.physletb.2014.06.058
- [48] R. Ruiz, JHEP **1512**, 165 (2015)

- doi:10.1007/JHEP12(2015)165
- [49] J. C. Collins, D. E. Soper and G. F. Sterman, Nucl. Phys. B **250**, 199 (1985). doi:10.1016/0550-3213(85)90479-1
- [50] R. E. Ruiz, *Hadron Collider Tests of Neutrino Mass-Generating Mechanisms*, Ph.D. thesis, University of Pittsburgh (2015)
- [51] A. Das, P. Konar and S. Majhi, arXiv:1604.00608 [hep-ph].
- [52] A. Alloul, N. D. Christensen, C. Degrande, C. Duhr and B. Fuks, Comput. Phys. Commun. **185**, 2250 (2014)
- [53] N. D. Christensen and C. Duhr, Comput. Phys. Commun. **180**, 1614 (2009)
- [54] C. Degrande, Comput. Phys. Commun. **197**, 239 (2015) doi:10.1016/j.cpc.2015.08.015
- [55] T. Hahn, Comput. Phys. Commun. **140**, 418 (2001) doi:10.1016/S0010-4655(01)00290-9
- [56] C. Degrande, C. Duhr, B. Fuks, D. Grellscheid, O. Mattelaer and T. Reiter, Comput. Phys. Commun. **183**, 1201 (2012) doi:10.1016/j.cpc.2012.01.022
- [57] R. Ruiz, “SM + Heavy N at NLO in QCD”, <http://feynrules.irmp.ucl.ac.be/wiki/HeavyN>
- [58] J. Alwall, R. Frederix, S. Frixione, V. Hirschi, F. Maltoni, O. Mattelaer, H.-S. Shao and T. Stelzer *et al.*, JHEP **1407**, 079 (2014)
- [59] K. A. Olive *et al.* [Particle Data Group Collaboration], Chin. Phys. C **38**, 090001 (2014). doi:10.1088/1674-1137/38/9/090001
- [60] R. D. Ball *et al.* [NNPDF Collaboration], Nucl. Phys. B **877**, 290 (2013) doi:10.1016/j.nuclphysb.2013.10.010
- [61] A. Avetisyan *et al.*, arXiv:1308.1636 [hep-ex].
- [62] M. Cacciari and G. P. Salam, Phys. Lett. B **641**, 57 (2006) doi:10.1016/j.physletb.2006.08.037
- [63] M. Cacciari, G. P. Salam and G. Soyez, Eur. Phys. J. C **72**, 1896 (2012) doi:10.1140/epjc/s10052-012-1896-2
- [64] M. Cacciari, G. P. Salam and G. Soyez, JHEP **0804**, 063 (2008) doi:10.1088/1126-6708/2008/04/063
- [65] T. Sjstrand *et al.*, Comput. Phys. Commun. **191**, 159 (2015) doi:10.1016/j.cpc.2015.01.024 [arXiv:1410.3012 [hep-ph]].
- [66] V. Hirschi and O. Mattelaer, JHEP **1510**, 146 (2015) doi:10.1007/JHEP10(2015)146
- [67] M. L. Mangano, M. Moretti, F. Piccinini and M. Treccani, JHEP **0701**, 013 (2007) doi:10.1088/1126-6708/2007/01/013
- [68] S. S. D. Willenbrock and D. A. Dicus, Phys. Lett. B **156**, 429 (1985). doi:10.1016/0370-2693(85)91638-7
- [69] T. Han, G. Valencia and S. Willenbrock, Phys. Rev. Lett. **69**, 3274 (1992) doi:10.1103/PhysRevLett.69.3274
- [70] T. Gleisberg, S. Hoeche, F. Krauss, M. Schonherr, S. Schumann, F. Siegert and J. Winter, JHEP **0902**, 007 (2009) doi:10.1088/1126-6708/2009/02/007
- [71] M. Ababekri, S. Dulat, J. Isaacson, C. Schmidt and C.-P. Yuan, arXiv:1603.04874 [hep-ph].
- [72] N. Arkani-Hamed, T. Han, M. Mangano and L. T. Wang, arXiv:1511.06495 [hep-ph].